Characteristics of ionospheric irregularities near the north EIA at 121 °E

Jinghua Li[1], Guanyi Ma[1,2], Klemens Hocke[3,4], Qingtao Wan[1], Jiangtao Fan[1], Xiaolan Wang[1]

[1] National Astronomical Observatories, Chinese Academy of Sciences, Beijing, China.

[2] University of Chinese Academy of Sciences, Beijing, China.

[3] Institute of Applied Physics, University of Bern, Bern, Switzerland

[4] Oeschger Centre for Climate Change Research, University of Bern, Bern, Switzerland

Corresponding to: G. Ma (guanyima@nao.cas.cn)

Abstract. Observation from two IGS stations TWTF (24.95 °N, 121.16 °E, dip latitude: 18.20 °N) and SHAO (31.10 °N, 121.20 °E, dip latitude: 23.30 °N) are used to study the characteristics of the irregularities. Five latitude belts, 20~23 °N, 23~26 °N, 26~29 °N, 29~32 °N and 32~35 °N are divided according to the latitudes of the ionospheric piercing points. The seasonal variation and the latitude dependence of the occurrence are studied for three different solar activity years of 2003 (medium year), 2008 (minimum year) and 2014 (maximum year). Local occurrence rate (LOR) is proposed and defined as the ratio of the number of ROTI larger than the threshold to the number of observed ROTI in the nighttime. It can indicate the spatiotemporal range of the irregularity. LOR in one month is calculated to research the irregularities together with the monthly occurrence rate (MOR), which is defined as the ratio of the irregularities traverse events to the observation days in one month. MOR in May/June is larger than those in equinoxes except in 20~23N for the March of 2014, which is different from the equinoctial occurrence maximum of equatorial plasma bubbles (EPB). In 20~23 °N and 23~26 °N, LOR maximum are observed in March and September, and no peak appeared in June. But in the higher three latitude belts, LOR maximum appeared in June. LOR and MOR peaks in March and September means the irregularities appeared frequently with large spatiotemporal range. Large MOR and small LOR in June in 20~23 °N and 23~26 °N implies the irregularities often occurred with small spatiotemporal range. In 26~29 °N, 29~32 °N and 32~35 °N, the maximum of MOR and LOR were in June, implying the irregularities appeared more frequently and had larger spatiotemporal range than those in other months. Moreover, MORs and LORs decrease with the latitudes in March and September of 2003 and 2014. This implies the EPB played an important role on the irregularities in these months. In June, MORs and LORs in the higher three latitudes belts are

larger than the lower two ones, it can be suggested that the irregularities in this month were mainly from the nonequatorial process, which is more frequently happened but weaker than plasma bubble in spatiotemporal scale. MOR, LOR and the ROTI maximum in each month are small in 2008. The seasonal variation of ROTI maximum proved that the irregularities in 29~32 °N and 32~35 °N has small TEC fluctuation in the three years. But they peaks in spring and autumn of 2003 and 2014 in 20~23 °N, 23~26 °N and 26~29 °N. This confirmed the results from MOR and LOR.

1 Introduction

The ionospheric irregularities are spatially irregular variation of electron density or fluctuation of total electron content (TEC) with scale lengths from a few meters to several tens of kilometers. When radio waves propagate through the irregularities, variations in signal strength happen due to refractive effect. This phenomenon is referred to as ionospheric scintillation, which degrades both the performance of satellite communication and the precision of satellite navigation (Basu & Basu, 1981; Maruyama, 2002). Severe scintillation can lead satellite service interruption due to loss of lock in receivers. Moreover, TEC fluctuations in ionospheric irregularities are a major error to radio interferometers, differential Global Positioning System (DGPS) and synthetic aperture radar (SAR) (Erickson et al., 2001; Zabotin and Wright, 2004; Afraimovich and Yasukevich，2008；Lee et al., 2011, Zheng et al., 2008).

Most intense ionospheric irregularities are those occurred in low-latitude regions near the magnetic equator. They were first recorded as the spreading of the traces of F layer echoes on ionograms with ionosonde. It has been since called equatorial spread F as well (Booker and Wells, 1938). Using the data from incoherent scattering radar, a plumelike irregular structure was found in a range-time-intensity diagram which provides the dynamic process of the irregularity evolution. It was then proposed that the irregularities are produced as low-density ‘plasma bubbles’ at the bottomside of the ionosphere and bubbles can easily reach even much more than 1000 km (Woodman and La Hoz, 1976). The equatorial plasma bubbles (EPB) were directly confirmed by AE-C satellite in-situ measurements as regions of abrupt drop-out of electron density by two orders of magnitude with sizes of several tens of kilometers (McClure et al., 1977). Furthermore the optical imaging techniques probed two-dimensional structure of the plasma bubble (Weber et al., 1978; Mendilo and Baumgardner, 1982; Balan et al., 2018). It has been generally understood that plasma bubbles are generated at the bottom of the equatorial ionosphere by the generalized nonlinear Rayleigh-Taylor instability. While moving upward from the lower ionosphere into the higher density ionosphere, they extend along the magnetic flux tube to higher latitudes and often reach to the equatorial ionization anomaly (EIA) crest (Kelley and McClure, 1981; Ossakow, 1981).

The ionospheric irregularities have been studied with radar, satellite, airglow imager observations and simulations (Balan et al., 2018). Different observational techniques have their own advantage to reveal different aspects of the characteristics of the ionospheric irregularity. Since the civilian use of Global Navigation Satellite System (GNSS) the observation with ground-based dual-frequency GNSS receivers has become an important mean for ionospheric studies. While the fluctuation of phase and amplitude of GNSS signal, and hence scintillation, occur due to ionospheric irregularity, TEC also fluctuates. The rate of change of the TEC, termed ROT, and further, a rate of TEC index (ROTI) have been proposed as an indicator of the presence of ionospheric irregularity and a parameter of TEC fluctuation (Aaron et al., 1996; Pi et al. 1997; Basu et al., 1999). ROTI was used to investigate extensively the ionospheric equatorial bubbles or irregularities at different time and over different regions for the last 20 years. Statistical and case studies were successful in describing the occurrence features of the irregularity with local time, seasonal variations, solar cycle and its geographical dependence (Otsuka et al., 2006, Nishoka et al., 2008; Sripathi et al., 2018). Mungufeni et al. (2016) studied the ionospheric irregularities over African low latitude region during quiet and disturbed geomagnetic conditions, and found the equinox asymmetries of the irregularities' strength. Nevertheless, the characteristics of the irregularities near EIA have not been fully understood. This area is located between the equator and the mid latitude, and the irregularities may be affected by different process.

This paper aims to study statistical characteristics of irregularities near the north EIA with continuous GPS observations for the solar minimum of 2008, medium of 2003 in the declining phase of cycle 23, and the solar maximum of 2014 in solar cycle 24. Section 2 describes observation and data analysis method. Section 3 gives the results. Section 4 deals with the discussion. Finally, conclusions are drawn in section 5.

2 Observation and data analysis

2.1 Observation

The observations are from two International GNSS Service (IGS) stations TWTF (24.95 °N, 121.16 °E, dip latitude: 18.20 °N) and SHAO (31.10 °N, 121.20 °E, dip latitude: 23.30 °N). The dual frequency GPS receivers at the two stations sample the measurements with 30-s intervals. TWTF is near the north EIA crest. SHAO station is ~6 degree higher in latitude than TWTF along the longitude. The data from SHAO is used to understand the characteristics of the low-latitude irregularities better at TWTF. The data are from the solar medium of 2003, minimum of 2008 in the declining phase of cycle 23, and the solar maximum of 2014 in solar cycle 24. For SHAO station, no measurement is recorded from the 193rd day except the 329nd day.

Figure 1 depicts a map of the ionospheric piercing point (IPP) of GPS satellites at 400 km observed from TWTF and SHAO, with an elevation cutoff of 30 degrees, during 18:00~06:00 local time on 20th March 2003. The starting positions of the traces are marked with dots. The coverage of these traces is mainly within 20-35 °N in latitude and 116-126 °E in longitude. The stars represent the location of the two receivers. The dash lines represent the magnetic latitude marked by the number on the right. Due to the periodic orbits of the satellites, the coverage of the IPP traces is almost the same every day. According to the latitude of IPPs, the area are divided into 5 latitude belts, 20-23 °N, 23-26 °N, 26-29 °N, 29~32 °N, 32~35 °N to study the dependence of the irregularities near the EIA crest.

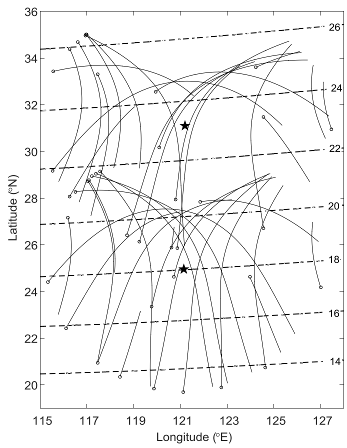

Figure 1 The IPP trace at the two stations

2.2 ROTI calculation

Dual-frequency GPS receiver recorded the phase measurements (L_1, L_2) on two frequency of 1.574GHz (referred as f_1) and 1.228GHz (referred as f_2) in the observation files at 30 sec interval. Based on the phase measurements, the relative slant TEC along the line of sight (LOS) between the satellite and receiver can be calculated. By taking the difference between the slant TECs at two successive times, a rate of change of the TEC was defined as $ROT_i = (N_{Ti} - N_{Ti-1})/(t_i - t_{i-1})$ where N_{Ti} is the slant TEC for the i^{th} measurement at time t_i (Aarons et al.，1996). Further, ROTI, the standard deviation of ROT, is calculated to quantify the TEC fluctuation by $ROTI = \sqrt{\langle ROT_i^2 \rangle - \langle ROT_i \rangle^2}$ in 5 minutes (Pi et al., 1997). The cycle slip of the phase measurements and loss of lock are detected when ROTI is calculated.

2.3 Detection of irregularity traverse event

The ionospheric irregularity is surveyed by a criterion as follows. The GPS observation with satellite elevation larger than 30 degrees is used in order to mitigate the effect of the multipath. A threshold is needed to detect the existence of the irregularity by ROTI. The threshold is calculated from the daytime (6:00LT~18:00LT) observations, considering that the irregularities often appear in the nighttime. It is defined as:

$$thrshld = median + 10 \times rms \tag{6}$$

Median and root mean square (RMS) of ROTI are from all of the ROTIs in one daytime. So the threshold is a little different day by day, and it varies in the range of 0.11-0.20 TECU/min for all the days in 2003, 2008 and 2014. If more than 20 consecutive ROTIs are larger than the threshold, the IPP is reckoned to traverse the ionospheric irregularities, and an irregularity traverse event is identified and the beginning time is marked by the first epoch with ROTI larger than the threshold. If more than 40 consecutive ROTIs in 20 minutes are smaller than the threshold, the ending time is marked as the first epoch when ROTI is smaller than the threshold. Another irregularity traverse event will be counted if it is encountered more than 1 hour later than the ending time of the previous event.

2.4 Occurrence rates definitions

Two kinds of occurrence rates are defined and studied. Monthly occurrence rate (MOR) is used to describe the frequency of the irregularity events in one month and defined as:

$$MOR = \frac{\text{the days with irregularity in one month}}{\text{all the observation day in the month}} \qquad (7)$$

Higher monthly occurrence rate implies the irregularity happens frequently in daily scale.

Local occurrence rate (LOR) is proposed to indicate the spatiotemporal range of the irregularities and are calculated by:

$$LOR = \frac{\text{the number of ROTIs larger than the threshold in events}}{\text{all the ROTIs number during the nighttime}} \qquad (8)$$

The duration of the irregularities and the numbers of IPP encountering the irregularities will affect the value of LOR, but they did not change MOR. The ionospheric irregularities with large spatiotemporal scales can result in large LOR. To compare with MOR, LOR is calculated in one month.

3 Results

3.1 Start time of irregularity traverse

The irregularities traverse events were detected by ROTI in the three years at TWTF and SHAO. The distribution of the beginning time for the irregularity events is shown in Fig. 2. The left panel is based on the observations at TWTF, and the right one is for SHAO station. At TWTF, most of the irregularity traverse events were first observed after sunset and before midnight. The occurrence time is not similar in the three years. In 2003, the occurrence number was large at 20:00~22:00 LT with the maximum at 20:00~21:00 LT. In 2008, the occurrence number increased with the local time before midnight and then it decreased, the maximum was at 23:00~00:00 LT. In 2014, the irregularities mainly appeared at 19:00~00:00 LT, and the maximum was at 19:00~20:00 LT. After midnight the occurrence number soon decreased.

At SHAO station, the irregularity events also mainly appeared before midnight, but no occurrence peaks appeared after sunset. The occurrence time varies in a similar way in the three years. The occurrence number gradually increased and peaked at 21:00~23:00 LT, and then it decreased. Compared the occurrence time at TWTF, the occurrence time at SHAO was later. The latitude of SHAO station is ~6 degree higher than the TWTF station. If the irregularities observed at TWTF and SHAO were from the equatorial plasma bubbles, they must be observed earlier at TWTF. If the irregularities are from the non-equatorial process, it depends on the source location of the irregularities. Based on the two stations observations, it is difficult to tell where the source of the irregularities is, and it is not the focus of this paper.

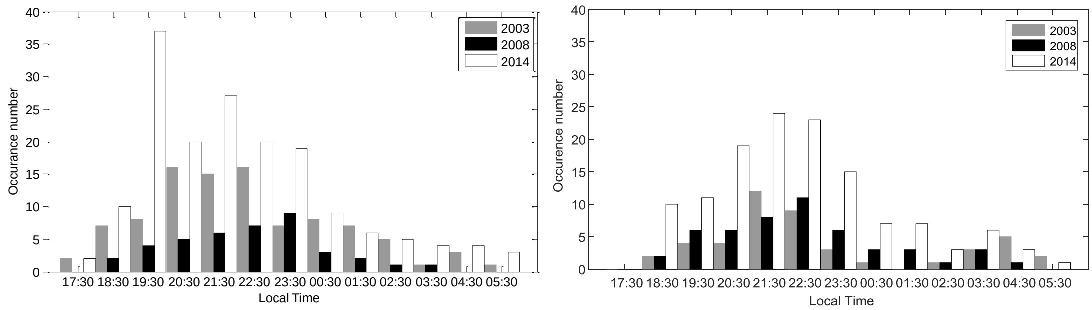

Fig. 2. Distribution of the first observed times for irregularity traverses at TWTF and SHAO.

3.2 Variation of MOR

In this section the seasonal variation and latitude dependence of MOR is studied for the three different solar activity years. MOR and LOR in August to December of 2003 are only based on the TWTF station because of the data outage at SHAO station.

Figure 3 presents the variation of MORs in 2014, 2003 and 2008 respectively. This figure shows that MORs in 2014 were generally larger than those in 2008 and 2003. In the solar maximum activity year of 2014, MORs for 20~23 °N peaked in March, June, September and November with the value of 67%, 57%, 37% and 15% respectively. For this latitude belt, MORs in March and June were larger than that in September and November. But in 23~26 °N MORs did not peak in winter, and the value of 61% in March was a little smaller than 64% in June. In 26~29 °N, 29~32 °N and 32~35 °N, MORs only peaked in March and June. And in these latitudes, MORs in June were 71%~82%, much larger than the values of 7%~32% in March.

In the medium solar activity year of 2003, the seasonal variation of MOR was very different from that in 2014. In 20~23 °N, MOR peaked in February, May and October with the value of 18%, 41% and 15% respectively. At 23~26 °N, MORs peaked in February, June and October with the value of 21%, 46% and 15% respectively. MORs in the higher three latitude belts peaked only in June with the value of 39%, 46% and 51%, which were much larger than the values in other months. This means the irregularities appeared more frequently in June in the medium solar activity year of 2003.

In the minimum solar activity year of 2008, the peaks appeared in May and June, which was similar to that in 2003. But in this year, MOR did not peak in autumn for all the latitude belts. In the lower three latitude belts, MORs had peaks of ~25% in May. In 29~32 °N and 32~35 °N, MORs peaked in June with the value of ~35%. Compared with those in 2003 and 2014, MORs were much smaller in 2008.

Besides the seasonal variations, MORs also depended on the latitudes, as shown in Figure 3. MORs decreased with the latitudes in March and September of 2014. Similar latitude dependence appeared in February and March of 2003. This means the irregularities appeared more frequency at the lower latitudes in these months. In June of the three years, MORs increased with the latitudes except that at 32~35 °N. This implies that the irregularities in June occurred more frequently in the higher latitudes.

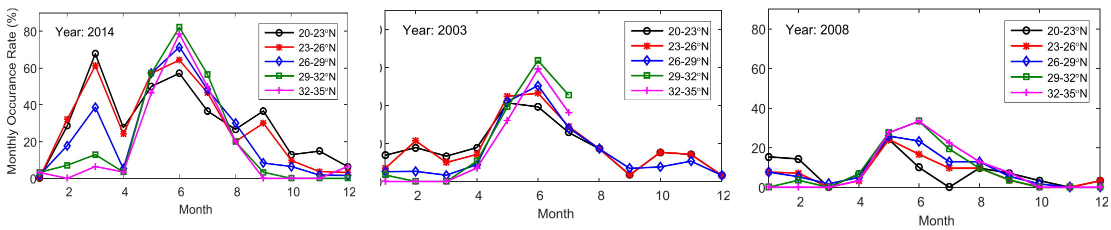

Figure 3 MOR of irregularities in 2008, 2003 and 2014 for different latitude belts

3.2 Variation of LOR

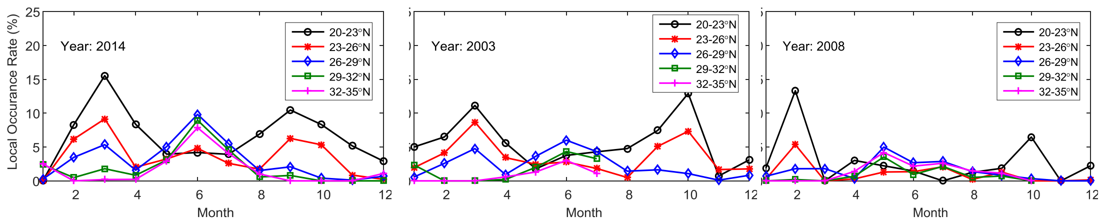

Figure 4 LOR of irregularities in 2003, 2008 and 2014 for different latitude belts

As mentioned in section 2, we defined LOR to describe the spatiotemporal variation of the ionospheric irregularities. Figure 4 shows LOR in each month for the three different solar activity years. In 2014, LORs for 20~23 °N peaked in March and September with the value of 16% and 11% respectively. Different from MOR, LOR did not peak in June in this year. This means the irregularities in this latitude belts had small spatiotemporal range although they appeared frequently. In 23~26 °N, LORs began to appear small peak of 4% in June, at the same time, the peaks in March and September were 9% and 6%. At the higher three latitude belts, the peaks of 8%~10% in June were larger than the values of 0~5% in March, and no peaks appeared in autumn. This implies the irregularities at 26~35 °N had larger spatiotemporal range in June than those in March.

In 2003, LORs had similar seasonal variation to those in 2014 besides that the autumn peaks were in October in 20~23 °N and 23~26 °N. In the solar minimum year of 2008, the two peaks of 14% and 7% were in February and October at 20~23 °N. At 23~26 °N, LOR peaks in February and July of 2008. LORs of 4%~5% in May were larger than those in other months for the latitude belts of 26~29 °N, 29~32 °N and 32~35 °N.

Compared Figure 4 with Figure 3, it can be noted that the MORs and LORs were different at different latitude belts. In March and September of 2014, March and October of 2003, and February of 2008, both MORs and LORs decreased with the increasing of the latitudes. This implies the irregularities were mainly from the equatorial plasma bubbles, and the equatorial plasma bubbles may play an important role in these months. In June of 2014, MORs increased with the latitudes except that at 32~35 °N, and LORs at the three higher latitude belts were close to each other, and they were larger than those at 20~26 °N. It suggested that the irregularities in June were not mainly from the equatorial process, the non-equatorial process played an important role on the summer irregularities. The latitude dependence of LOR in June of 2003 was not same to that in 2014, but they were similar to each other and different with the characteristics of the equatorial plasma bubbles.

3.3 Variation of ROTI Maximum

As mentioned above, ROTI is an index to dedicate the fluctuation of TEC. Therefore, large ROTI means large electron density fluctuation. Figure 5 displays the variation of the monthly ROTI maximum for different latitude belts in the three different solar activity years. ROTI maximum tends to be larger for higher solar activity.

In solar maximum year of 2014, ROTI maximum in 26-29 °N and 26-29 °N were less than 2.0 TECU/min in the whole year. ROTI maximum had peaks of 7.8-8.9 TECU/min in Feb/Mar and 2.2-4.90 TECU/min in Sep for the latitude belts of 20-23 °N, 23-26 °N and 26-29 °N. The largest ROTI maximum happened in the latitude belt of 23-26 °N in March and September. In February, ROTI largest maximum appeared at 26~29 °N. In June and the peak value of 2.2 TECU/min for latitude belt 26-29 °N was comparatively large, and values of ~1.0TECU/min in other latitude belts were close to each other. The ROTI maximum at latitude belt 20-23 °N had a moderate peak of 4.5 TECU/min in November. There were also peaks in September, although the values of ROTI maximum were around 3.84 TECU/min, which is smaller than that in May. ROTI maximum in 26-29 °N latitude belt was generally smaller than those in 20~23 °N and 23~26 °N latitude belts for the whole year except in June.

In solar medium year of 2003, ROTI maximum in the lower three latitude belts generally peaked at Feb/Mar and October with values of ~3.9-7.6 TECU/min and ~1.8-3.4 TECU/min, respectively. ROTI maximum for latitude belt 20-23 °N also has peaks in May, August and October. The ROTI maximum increased with latitude in March, it can also decrease with latitude in April-August and October for the lower three latitudes. And in the higher two latitude belts, ROTI maximum peaks in summer and the values are ~1.0TECU/min.

In solar minimum year of 2008, the ROTI maximum was very low and peaked in February and October with values of 1.7 and 1.2 TECU/min for latitude belts 20~23 °N. In 23~26 °N, the peak 1.5 TECU/min only appeared in February. In 26~29 °N the maximum peaks in June with the value of 1.6 TECU/min. It was around or below 0.50 TECU/min for other months. The differences of ROTI maximums among different latitude belts were generally small.

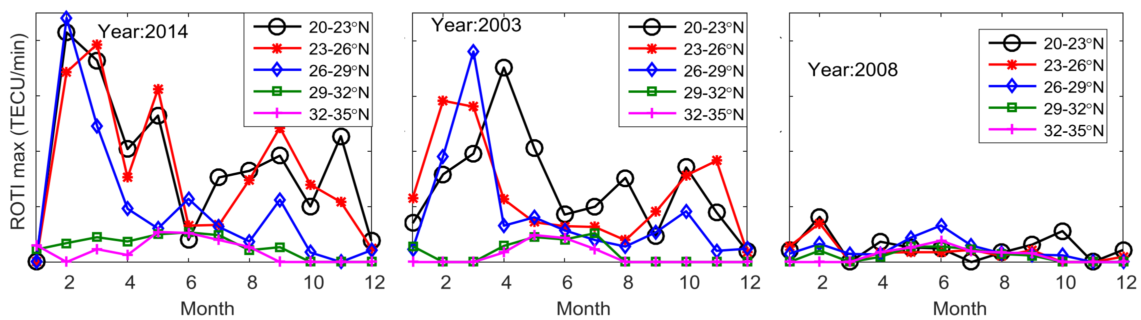

Figure 5 variation of ROTI maximum

3.4 ROTI maximum with solar activity

A scatter plot was presented to tell the relation of ROTI maximums for each the irregularity traverse event with solar activity, as shown in Fig. 6. Here used is the radio flux at 10.7 cm (F10.7) as an indicator of the solar activity. The symbols of cross, circle and dot represent the year of 2003, 2008 and 2014, respectively. The colors in red, magenta, green and blue distinguish spring, summer, autumn and winter.

In solar minimum of 2008, F10.7 was smaller than 80 sfu. At TWTF ROTI was generally around 0.50 TECU/min in this year, and the largest ROTI was 1.64 TECU/min in winter. At SHAO, most ROTI was around 0.3 TECU/min, and the maximum was in summer. In solar medium and maximum years of 2003 and 2014, F10.7 was between 84-172 sfu and 86-208 sfu, respectively. At TWTF, the ROTI maximum had a tendency to increase with F10.7. However, ROTI can be small (less than 1 TECU/min) no matter how large F10.7 is. At SHAO, ROTI did not have relation to F10.7in all the seasons of the three years, and ROTI values were much smaller than those at TWTF.

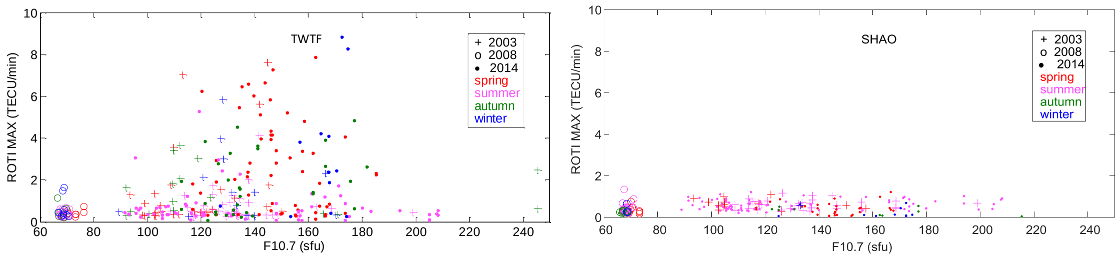

Fig. 6. Scatter plot of ROTI maximum for irregularity event versus F10.7 for different solar activity years.

4 Discussions

Low latitude irregularities are generally thought to be related with plasma bubbles generated at the magnetic equator. The occurrence of EPB in Asian region is known to be maximum in equinoxes (Tsunoda, 1985). Nishioka et al. (2008) revealed higher MOR of EPBs around spring equinox (summer solstice) than autumn equinox (winter solstice) from 2000 to 2006 with ground-based GPS networks around the dip equator. In Fig. 3, the MORs in solar maximum year of 2014 generally showed maximum values in March, June, September, and November, respectively. The maximum value in March (June) was much larger than that in September (November) for latitudes 20-26 °N. This is in agreement with the results from GPS observations both at equatorial region and crest in solar maximum and high activity years (Nishioka et al., 2008; Kumar, 2017; Lee et al., 2009). But the MOR peaks in November only appeared in 20~23 °N. In the higher latitude belts, no MOR peaked in winter. This implies the irregularities near the dip equator in winter solstice cannot reach the latitudes higher than 23 °N.

In a morphology study of EPBs during low and high solar activity years in latitudes 13-17 °N over Indian sector, Kumar (2017) found maximum EPB occurrences during the equinoctial months throughout 2007–2012 except during the solar minimum years in 2007–2009. During 2007–2009, the maximum EPB occurrences were observed in June solstice. However, Figure 3 shows that the MOR in June are generally higher than that in equinoxes except at 20~23 °N in 2014. In 2003, MOR of the irregularities in June is also higher than those in March and September. This is different from the occurrence of the EPBs in the high and medium solar activity years (Kumar, 2017). The difference should mainly owe to the higher latitudes in this paper than those used by Kumar (2017). The effect of the EPBs decreases with the latitudes in the equinoctial months, and at the latitude higher than ~26 °N, the MOR in the equinoctial months is low.

Lee et al. (2009) investigated the occurrence probabilities of irregularity in solar maximum of 2000 at Chungli (24.9 °N, 121.2 °E) and (14.0-14.6 °N, 121.0-121.1 °E) in Manila. They found that the seasonal variations at the crest and the dip equator had similar trends. They also showed the range spread F (RSF) had similar occurrence probability to that of GPS phase fluctuations while the frequency spread F (FSF) peaked in June as the spread F at mid latitude. The seasonal variation in this paper for the two lower latitude belts in 2014 is consistent to their observations in 2002. The high MOR in June is similar to the FSF. Using the observation in Japan in 2000, Otsuka et al. (2006) showed similar results that the occurrence rate peaks at equinoxes in 25 °N, but peaks at summer in 29 °N. The peaks in 25 °N is because of the latitudes of Japan.

In both solar medium 2003 and minimum 2008, the MOR just shows maximum values in May/June. MOR in the higher three latitude belts of 26-29 °N, 29-32 °N and 32-35 °N are larger than those in the two lower ones. This implies that the irregularity is encountered more frequently at higher latitude. Kumar (2017) also reported maximum MOR in June observed with GPS receivers in latitudes 13-17 °N over India for 2007-2009. However, Buhari et al. (2017) found that the MOR of EPBs over Malaysia (near magnetic equator, 1~7 °N in geolatitude) was still active during equinoctial months in low solar activity years. In this paper, the irregularities in 2008 did not show high occurrence in the equinoctial months for all the latitudes. Maybe the EPBs near the magnetic equator in the low solar activity years are weak and cannot reach the latitude of 20 °N.

LOR is a parameter to represent the spatiotemporal range of the irregularities. It is used to describe another characteristic of the irregularities in this study. In 2014 and 2003, LOR peaks in March and September/October for the latitude belts of 20~23 °N and 23~26 °N. This means the irregularities in the two latitude belts has larger spatiotemporal range than those in other months. While for the latitude belts of 26~29 °N, 29~32 °N and 32~35 °N, LOR in May/June are larger than those in spring and autumn. Compared the seasonal variation of MOR with LOR, it can be seen the spatiotemporal range of the irregularities in summer is small although the monthly occurrence is high in these months.

Nonequatorial processes were also suggested by Sripathi (2018) for equatorial and low latitude irregularities, which showed that the postmidnight spread F during summer was weaker in strength and shorter in duration than equatorial spread F mostly occurred in equinoxes and winter. Further the postmidnight spread F during summer is found to be stronger and earlier at low latitudes followed by their occurrence at the equator (Sripathi et al., 2018). The EPBs-induced irregularities can reach different latitudes from the dip equator in different events; therefore, the occurrence of these irregularities must decrease with latitudes in statistics. Otherwise, the irregularities are not from the EPBs, which are referred as non-equatorial process. MORs and LORs decrease with the latitudes in spring and autumn of 2014 and 2003, February and October of 2008. This means the irregularities in these months are mainly from the EPBs. But in summer, MOR and LOR did not decrease with the latitudes. They are smaller in 20~23 °N and 23~26 °N than those in three higher latitude belts. The irregularities may be mainly affected by the nonequatorial process. The nonequatorial process did not affect the lower latitude irregularities in 20~23 °N and 23~26 °N obviously.

Figure 5 shows the variation of the ROTI maximum. In the solar minimum of 2008, the ROTI maximum is quite weak for the whole year compared with that in 2014. Higher solar activity implies greater pre-reversal eastward electric field, earlier occurrence and earlier decay of EPBs under magnetically quiet conditions (Fejer et al., 1999; Hysell et al., 2002). In solar medium and maximum the irregularity associated with plasma bubble can be very strong not only in March, but also in Feb and April. The ROTI maximum in May to August in 2003 is the smallest in latitude belt 26-29 °N, implying that the irregularity originated in nonequatorial processes is much weaker than plasma bubble. The small ROTI maximum and LOR in 29-32 °N and 32-35 °N in these months confirm this suggestion again. It is known that Perkins instability is responsible for the mid latitude irregularities (Perkins, 1973; Yokoyama et al., 2009). Otsuka et al. (2006) observed that the frequent occurrence of the irregularity in mid latitude in the summer night was usually accompanied by medium-scale traveling ionospheric disturbances (MSTID). Meridional observations from mid latitude to magnetic equator are needed to confirm and clarify the nonequatorial origin of the irregularities observed near equatorial anomaly crest. Because of the limitation of the IGS station, no observations near the magnetic equator are obtained along the longitude of 121E. Further study will be explored for other meridional observations.

The scatter plot of ROTI maximum versus F10.7 is rather dispersed, as shown in Fig. 6. However, confined in a funnel, a large ROTI maximum has a tendency to be related with a large F10.7. But the reverse is not always true. Higher solar activity only is a necessary condition for the production of stronger plasma bubble related irregularities.

5. Conclusion

Using the GPS observations at TWTF (24.95 °N, 121.16 °E, dip latitude: 18.20 °N) and SHAO (31.10 °N, 121.20 °E, dip latitude: 23.30 °N), characteristics of the ionospheric irregularities near the EIA crest are studied for the solar minimum of 2008, medium of 2003 and the solar maximum of 2014. The irregularity events were detected with ROTI. Most of the irregularity events were first observed after sunset and before midnight. The maximum occurrence time is between 19:00~20:00 LT in 2014. Local occurrence rate (LOR) is proposed to describe the spatiotemporal range of the irregularities. The monthly occurrence rate (MOR), LOR and ROTI maximum are analyzed in five latitude belts of 20-23 °N, 23-26 °N, 26-29 °N, 29-32 °N and 32-35 °N.

In 2003 and 2014, MORs peaked in February/March, May/June and September/October for the latitude 20~23 °N and 23~26 °N. For the latitude 26~29 °N, no MOR peak appeared in autumn of 2014, and in 2003 MOR only peaked in June. The MORs of the irregularities observed in 20-23 °N, 23-26 °N were similar to the occurrence of the EPBs in 2003 and 2014. As for LOR in 20-23 °N and 23-26 °N, obvious equinox peaks appeared in 2003 and 2014, and no LOR peak was observed in June. For the higher three latitude belts, the LOR maximum appeared in June of 2003 and 2014. MORs and LORs decreased with latitudes in the March and September/October of the two years. This indicated the irregularities were mainly from the EPBs. In June of 2003 and 2014 MORs and LORs for the higher three latitude belts are larger than the low two ones, which imply the nonequatorial process played an important role on the irregularities. In 2008, LOR peaks only appeared in February (20-23 °N and 23-26 °N) and October (20-23 °N). MORs and LORs in this year were smaller than those in 2003 and 2014. The seasonal variation of ROTI maximum confirmed that the irregularities with large TEC fluctuation appeared in the equinoctial months for the lower latitudes. In the higher latitudes, they had small TEC fluctuation. Higher solar activity is a necessary but not sufficient condition for the production of stronger electron density irregularities.

Acknowledgement

This research has been carried out under the support of the National Natural Science Foundation of China (NSFC No. 11873064) and National key Research Program of China "Collaborative Precision Positioning Project" (No.2016YFB0501900). IGS is acknowledged for free use of GPS data. GM wishes to thank T. Maruyama for helpful discussion.

References

Aarons, J.: Global morphology of ionospheric scintillations, Proceedings of the IEEE, 70, 360-378, 1975.

Aarons, J., Mendillo, M., and Yantosca, R.: GPS phase fluctuations in the equatorial region during the MISETA 1994 campaign, Journal of Geophysical Research: Space Physics, 101, 26851-26862, 1996.

Abdu, M.A., Alam Kherani, E., Batista, I.S., de Paula, E.R., Fritts, D.C. and Sobral, J.H.A.: Gravity wave initiation of equatorial spread F/plasma bubble irregularities based on observational data from the SpreadFEx campaign, Annales Geophysicae, 27, 2607-2622, doi:10.5194/angeo-27-2607-2009, 2009.

Afraimovich, E.L. and Yasukevich, Yu.V.: Using GPSGLONASSGALILEO data and IRI modeling for ionospheric calibration of radio telescopes and radio interferometers, Journal of

Atmospheric and Solar-Terrestrial Physics, 70, 1949-1962, 2008

Balan, N., Liu, L. B., and Le, H. J.: A brief review of equatorial ionization anomaly and ionospheric irregularities, Earth and Planetary Physics, 2, 257–275, 2018.

Basu, S. and Basu, S.: Equatorial scintillations—a review, Journal of Atmospheric and Terrestrial Physics, 43, 473-489, 1981.

Basu, S., Groves, K.M., Quinn, J.M., and Doherty, P.: A comparison of TEC fluctuations and scintillations at Ascension Island, Journal of Atmospheric and Solar-Terrestrial Physics, 61, 1219-1226, 1999.

Booker, H. G., and Wells, H. W.: Scattering of radio waves by the f-region of the ionosphere, Journal of Geophysical Research, 43, 249-256, 1938.

Buhari, S. M., Abdullah, M., Yokoyama, T., Otsuka, Y., Nishioka, M., Hasbi, A. M., Bahari, S. A., and Tsugawa, T., Climatology of successive equatorial plasma bubbles observed by GPS ROTI over Malaysia, Journal of Geophysical Research: Space Physics, 122, doi:10.1002/2016JA023202, 2017

Erickson, W. C., Perley, R. A., Flatters, C., and Kassim, N. E.: Ionospheric corrections for VLA observations using local GPS data, Astronomy and Astrophysics, 366, 1071–1080, doi:10.1051/0004-6361:20000359, 2001.

Fejer, B. G.; Scherliess, L.; Paula, E. R. D. Effects of the vertical plasma drift velocity on the generation and evolution of equatorial spread F, J. Geophys. Res., 104(A9):19859-19869, 1999.

Hysell, D. L.; Burcham, J. D. Long term studies of equatorial spread F using the JULIA radar at Jicamarca, J. Atmospheric and Solar-Terrestrial Phys., 64(12-14):1531-1543. 12, 2002.

Kelley, M. C., and Mcclure, J. P.: Equatorial spread-F: A review of recent experimental results, Journal of Atmospheric and Terrestrial Physics, 43, 5, 427-435, 1981.

Kumar, S.: Morphology of equatorial plasma bubbles during low and high solar activity years over Indian sector, Astrophysics and Space Science, 362, 5, 93, 2017.

Lee, C. C., Chu, F. D., Chen, W. S., Liu, J. Y., Su, S.-Y., Liou Y. A., and Yu, S. B.: Spread F, GPS phase fluctuations, and plasma bubbles near the crest of equatorial ionization anomaly during solar maximum, Journal of Geophysical Research: Space Physics, 114, A08302, doi:10.1029/2009JA014195, 2009.

Lee, J., Amt, T. T., Jung, S., and Pullen, S.: Enhancements of Long Term Ionospheric Anomaly Monitoring for the Ground-Based Augmentation System, Proceedings of the 2011 International Technical Meeting of The Institute of Navigation, 930 San Diego, CA, January 24-26, 930-941, 2011.

Maruyama, T.: Ionospheric irregularities, Journal of the National Institute of Information and Communications Technology, 49, 163-179, 2002.

McClure, J. P., Hanson, W. B., and Hoffman, J. H.: Plasma bubbles and irregularities in the equatorial ionosphere, Journal of Geophysical Research: Space Physics, 82, 2650-2656, 1977.

Mendillo, M., and Baumgardner, J.: Airglow characteristics of equatorial plasma depletions, Journal of Geophysical Research: Space Physics, 87, 7641-7652, 1982.

Mendillo, M., Lin, B., and Aarons, J.: The application of gps observations to equatorial aeronomy, Radio Science, 35, 3, 885-904, 2000.

Mungufeni, P., Habarulema J. B., Jurua E.: Modeling of ionospheric irregularitiesduring geomagnetically disturbed conditions over African low-latitude region, Space Weather, 14, doi:10.1002/2016SW001446, 2016

Mungufeni, P., Habarulema J. B., Jurua E.:Trends of ionospheric irregularities over African low latitude region during quiet eomagnetic conditions, Journal of Atmospheric and Solar-Terrestrial Physics, 138-139, 261-267, 2016

Nishioka, M., Saito, A., and Tsugawa, T.: Occurrence characteristics of plasma bubble derived from global groundbased GPS receiver networks, Journal of Geophysical Research: Space Physics, 113, A05301, doi:10.1029/2007JA012605, 2008.

Ossakow, S. L.: Spread-F theories–A review, Journal of Atmospheric and Solar-Terrestrial Physics, 43, 437-443, 1981.

Otsuka, Y., Aramaki, T., Ogawa, T., and Saito, A.: A statistical study of ionospheric irregularities observed with a GPS network in Japan, Corotating Solar Wind Streams and recurrent Geomagnetic Activity, Geophysical Monograph Series, AGU, Washington, D. C., 2006.

Perkins, F.: Spread F and ionospheric currents, Journal of Geophysical Research: Space Physics, 78, 218–226, 1973.

Pi X., Mannucci, A. J., Lindqwister, U. J., and Ho, C. M.: Monitoring of global ionospheric irregularities using the worldwide GPS network, Geophysical Research Letters, 24, 2283-2486, 1997.

Sripathi, S., Sreekumar, S. and Banola, S.: Characteristics of Equatorial and Low-Latitude Plasma Irregularities as Investigated Using a Meridional Chain of Radio Experiments Over India, Journal of Geophysical Research: Space Physics, 123, 9, DOI: 10.1029/2017JA024980, 2018.

Weber, E. J., Buchau, J., Eather, R. H., and Mende, S. B.: North-south aligned equatorial airglow depletions, Journal of Geophysical Research: Space Physics, 83(A2), 712-716, 1978.

Woodman, R. F. and La Hoz, C.: Radar observations of F region equatorial irregularities, Journal of Geophysical Research: Space Physics, 81, 5447-5466, 1976.

Yokoyama, T., Hysell, D. L., Otsuka, Y., and Yamamoto, M.: Three-dimensional simulation of the coupled Perkins and Es-layer instabilities in the nighttime midlatitude ionosphere, Journal of Geophysical Research: Space Physics, 114, A03308, doi:10.1029/2008JA013789, 2009.

Zabotin, N. A., and Wright, J. W.: Phase structure functions for ionospheric radio sounding: Dependence on irregularity scale, Radio Science, 39, RS2003, doi:10.1029/2003RS002882, 2004.

Zheng, H., Li, L. and Li, F.: Study about Ionospheric Effects on Spaceborne SAR Azimuth Imaging, Journal of electronics & information technology (in Chinese), 30: 2085-2088, 2008